Virchows Archiv (2021) 479:133–145
https://doi.org/10.1007/s00428-021-03022-8

ORIGINAL ARTICLE

Mantle cell lymphomas with concomitant *MYC* and *CCND1* breakpoints are recurrently TdT positive and frequently show high-grade pathological and genetic features

Sietse M. Aukema[1,2] · Giorgio A. Croci[2,3] · Susanne Bens[4] · Kathrin Oehl-Huber[4] · Rabea Wagener[4,5] · German Ott[6] · Andreas Rosenwald[7] · Philip M. Kluin[8] · Eva van den Berg[9] · Anneke G. Bosga-Bouwer[9] · Mels Hoogendoorn[10] · Eva Hoster[11,12] · Iris Bittmann[13] · Inga Nagel[1,14] · Eva M. Murga Penas[1] · Markus Kreuz[15] · Julia Bausinger[4] · Wilfried Belder[16] · Ilske Oschlies[2] · Martin J. S. Dyer[17] · Sandrine Jayne[17] · Reiner Siebert[1,4] · Wolfram Klapper[2]

Received: 15 September 2020 / Revised: 28 December 2020 / Accepted: 6 January 2021 / Published online: 2 February 2021

Abstract

Chromosomal breakpoints involving the *MYC* gene locus, frequently referred to as *MYC* rearrangements (*MYC* − R+), are a diagnostic hallmark of Burkitt lymphoma and recurrent in many other subtypes of B-cell lymphomas including follicular lymphoma, diffuse large B-cell lymphoma and other high-grade B-cell lymphomas and are associated with an aggressive clinical course. In remarkable contrast, in MCL, only few *MYC* − R+ cases have yet been described. In the current study, we have retrospectively analysed 16 samples (*MYC* − *R*+, *n* = 15, *MYC* − *R*−, *n* = 1) from 13 patients and describe their morphological, immunophenotypic and (molecular) genetic features and clonal evolution patterns. Thirteen out of fifteen *MYC* − R+ samples showed a non-classical cytology including pleomorphic (centroblastic, immunoblastic), anaplastic or blastoid. *MYC* translocation partners were IG-loci in 4/11 and non-IG loci in 7/11 analysed cases. The involved IG-loci included IGH in 3 cases and IGL in one case. *PAX5* was the non-IG partner in 2/7 patients. The *MYC* − R+ MCL reported herein frequently displayed characteristics associated with an aggressive clinical course including high genomic-complexity (6/7 samples), frequent deletions involving the *CDKN2A* locus (7/10 samples), high Ki-67 proliferation index (12/13 samples) and frequent P53 expression (13/13 samples). Of note, in 4/14 samples, SOX11 was not or only focally expressed and 3/13 samples showed focal or diffuse TdT-positivity presenting a diagnostic challenge as these features could point to a differential diagnosis of diffuse large B-cell lymphoma and/or lymphoblastic lymphoma/leukaemia.

Keywords MYC · Mantle cell lymphoma · MCL · Blastoid · Terminal deoxynucleotidyl transferase · TdT · SOX11 · CDKN2A · TP53 · P53 · Clonal evolution

Introduction

In the diagnostic work-up of lymphoid neoplasms, especially those with pleomorphic or blastic morphology, expression of cyclin D1, SOX11 and terminal deoxynucleotidyl transferase (TdT), as well as *CCND1*-, *MYC*- and *BCL2*-chromosomal breakpoints, are diagnostic hallmarks of disease. Mantle cell lymphoma (MCL) typically presents as a lymphoid proliferation of medium-sized cells with centrocyte-like morphology and overexpression of cyclin-D1 as a result of an IG-*CCND1* juxtaposition. A subset of MCL presents with a pleomorphic or blastoid morphology resembling diffuse large B-cell lymphoma (DLBCL) or lymphoblastic lymphoma [1, 2]. Chromosomal translocation breakpoints involving the *MYC*

Sietse M. Aukema, Giorgio A. Croci, Reiner Siebert and Wolfram Klapper contributed equally to this work.

✉ Sietse M. Aukema
smaukema@gmail.com

✉ Reiner Siebert
reiner.siebert@uni-ulm.de

✉ Wolfram Klapper
wklapper@path.uni-kiel.de

Extended author information available on the last page of the article

gene locus, commonly referred to as *MYC* − rearrangements (*MYC*-R+) and characteristic of Burkitt lymphoma [3], have been occasionally detected in low-grade follicular lymphoma [4–6] but are more frequent in DLBCL and other high-grade B-cell lymphomas and are associated with an aggressive clinical course [7]. Compared to other high-grade B-cell lymphomas, *MYC* − rearrangements in MCL seem to be rare with so far only few cases being reported including a series of 17 cases published by Hu et al. [8, 9] In another series, Wang et al. reported the presence of a *MYC* − break to be an independent prognostic factor. [10] MCL with a *MYC* − break may present a diagnostic challenge since their morphology and immunophenotype are often atypical. In line with this, in the series published by Hu et al. [9], only 25% of MCL with *MYC* − rearrangement was unequivocally SOX11 positive. Along the same lines, a case of MCL with both *CCND1*− and *MYC* − breaks published by Kallen et al. [11] expressed TdT, the expression of which in the B-cell lineage is normally restricted to precursor B-cells in the bone marrow, precursor B-cell neoplasms, AML-M0 and rare high-grade B-cell lymphomas [12–14]. In the present study, we report on 15 *MYC* − R+ MCL samples from 13 patients and describe their morphological, immunophenotypic, (molecular) cytogenetic and molecular features and their clonal evolution patterns.

Methods

Case selection

All cases with *CCND1* and *MYC* breaks were retrieved from reference pathology and/or genetic laboratories, mostly in a retrospective manner. Analysis of *MYC* − break status was not routinely performed in MCL but was limited to cases with unusual morphological and/or immunophenotypical characteristics or with a 8q24 breakpoint in the karyotype. This includes cases morphologically and/or immunophenotypically favouring a diagnosis of DLBCL or high grade B-cell lymphoma during diagnostic workup (e.g. centroblastic, immunoblastic, lymphoblastic or Burkitt-like morphology, MYC positivity, SOX11 negativity and very high proliferative index). Cases with *MYC* gain, amplification or 8q24 breakpoint in the karyotype but without a *MYC* − break as determined by FISH with *MYC* break-apart and/or dual-/tri-colour fusion assays were not included. To be confident about the diagnoses of the cases and to avoid inclusion of plasma cell dyscrasias harbouring *CCND1* − rearrangements (e.g. multiple myeloma, plasma cell leukaemia), we did not include cases with only (conventional) cytogenetics but without any accompanying clinical, histopathological, immunohistochemistry (IHC) and/or flow-cytometry (FCM) information. Unless stated otherwise, the number of samples refers to *MYC* − R+ samples.

Immunohistochemistry and immunofluorescence

Immunohistochemistry was performed according to standard protocols [15, 16]. Specifically, staining protocols for Ki-67, SOX11, P53 and TdT have been published previously [12, 17–19]. With regard to scoring, SOX11 was scored as negative (0% positive lymphoma cells, score '0'), low (1–10%, score '1') or positive (> 10%, score '2'). P53 was scored as negative (0% positive lymphoma cells, score '0'), low (1–10%, score '1'), intermediate (10–50%, score '2') or high (> 50%, score '3') [18]. Immunofluorescence for 2-colour double staining on formalin-fixed paraffin embedded (FFPE) slides was performed with antibodies against TdT (1:10 diluted, clone SEN28, NovoCastra/ Leica, Wetzlar, Germany), CCND1 (cyclin-D1: (1:10 diluted, rabbit, Clon SP4, Thermo Scientific, Waltham, Massachussets, USA)), Alexa 488 and Alexa 555 labelled secondary antibodies (Thermo Scientific, Waltham, Massachussets, USA) on two TdT-positive cases (cases 5 and 6-R) with available material.

Conventional cytogenetics and molecular cytogenetics

Conventional and molecular genetic analyses were performed as previously described [12, 15, 16] and karyotypes were revised according to the ISCN 2016 nomenclature [20]. Complex karyotypes were defined as having ≥ 3 aberrations (including the *MYC* − translocation) [21]. FISH was performed using commercially probes: LSI *BCL2* BAP (18q21), LSI *BCL6* BAP (3q27), LSI *CCND1* BAP (11q13), LSI *MYC* BAP (8q24) and LSI IGH/*CCND1* (14q32/11q13), LSI IGH/*BCL2* (14q32/18q21) and LSI IGH/*MYC* (CEP8) (14q32/8q24 (8cen)) (all Abbott-Vysis, Downers Grove, IL, USA). In addition, non-commercial FISH assays for the detection of far telomeric/centromeric *MYC* breakpoints and IGK/*MYC* (2p12/8q24), IGL/*MYC* (22q11/8q24), *BCL6*/*MYC* (3q27/8q24) and *PAX5*/*MYC* (9p13/8q24) were applied [12, 15, 16, 22],

Copy number variant analysis

DNA extraction and copy number variant (CNV) analysis using the OncoScan™ CNV FFPE assay and array-CGH were performed on formalin-fixed paraffin embedded and frozen sections as previously described [12, 15] with the modification that for visual inspection of CNV's and regions of LOH, the Chromosome Analysis Suite (ChAS) software V4.0 was used (Affymetrix, Santa Clara, CA). For data visualisation of Fig. 2, the ChAS plug-in Multi Sample Viewer (MSV) was applied. Array-CGH data were already available for case 1 [15] and the genome annotations were lifted-over from hg17 to GRCh37/hg19 using the Lift Genome Annotations Tool of the UCSC Genome Browser (GRCh37/

Table 1 Immunohistochemical and molecular (cyto)genetic findings in mantle cell lymphomas with *CCND1* and *MYC* breaks

Immunohistochemical findings

No	Sex, age	Site	Cyto	cyclin-D1	SOX-11	P53	Ki-67	CD5	CD10	BCL6	MYC	TdT
1	M, 65	LN	Pleo, P-CB	+	2	1	50	+	+	-	80	-
2	M, 69	Sp	C	+	2	1	18	+	-	-	30	-
2-R1	+ 27Mo	BMB	C	+	2	3	53	+	-	-	40	-
2-R2[¶¶]	+ 52Mo	Skin	B	+	2	3	90	+	-	-	95	-
3	M, 60	BM[***,†††]	Pleo, IB/CB	+	0	2	80	-	-	+/-	40	-
4	M, 81[‡‡‡]	Stomach	B	+	2	3	95	-/+	-	NA	95	+ 20%
5	M, 71	LN	Pleo, anaplastic cells	+	2	2	70	+	-	-/+	90	≤2%
6	M, 53	LN	Pleo	+	2	2	54	+	-	-	80	-
6-R	+ 45Mo	Intra-dural	B	+	1	3	77	+	< 10%	-	90	< 5%
7	M, 64	BMB	Small cell	+	0	1	na	-	-	-	10[****]	-
8	M, 70	LN	Pleo, IB/CB	+	2	2	47	+	+	+	80	-
9	M, 83	LN	B	+	2	3	29	+	-	+	90	-
10	M, 58	Soft tissues	B	+	2	NA	86	+	NA	+	NA	NA
11	F, 65	Liver	B	+	1	2	95	+	-	+	90	-
12	M, 79	Skin	B	+	2	3	80	+	+	-/+	90	-
13	F, 77	PB[§§§§]	B	NA	NA	NA	NA	+/-	+/-	NA	NA	NA

	Conventional and/or molecular cytogenetic features[*]			Array-based CNV analysis[*,†]		
No	*CCND1*[‡]	*MYC*[§,¶]	Other	CN gain	CN loss	CNN-LOH
1	Pos	Break, *MYC-PAX5*	*BCL2* neg, *BCL6* neg	2p25.3-q13, 2q35-q37.3, 3p26.3-p24.1, 7p14.2-q36.3, 8q24.21-q24.3, 13q31.2-q34	8p23.3-q12.1, 9p24.3-p13.2, 9q33.3-q34.3, 13q14.2-q14.3, 15p13-q21.1	NA[**]
2	Pos	Neg	[††]nuc ish 3q27 (*BCL6* prox × 2, *BCL6* dist × 2), 11 (CEP11 × 2, *CCND1* × 3, *ATM* × 1, *FDX* × 1), 14q32 (IGH × 3, IGH prox × 2, IGH dist × 2), 17 (*P53* × 2, CEP17 × 2), (*BCL6* prox sep *BCL6* dist × 0)(IGH con *CCND1* × 2) (IGH prox sep IGH dist × 1)[‡‡]		11q22.2-q23.3	
2-R1	Pos	Break	46,XY,del(2)(p13p21),der(11)t(11;14)(q13;q32), der(14)t(14;19)(q32;q13),der(19)t(14;19)t(11;14)[2]/46,idem,t(8;18)(q24;q12),t(10;13)(p12;q14)[16]/46,XY[6] nuc ish(5′*MYC*,3′*MYC*) × 2(5′*MYC* sep 3′*MYC*x1), (*CCND1*,*IGH*)x3(*CCND1* con *IGH*x2), (*MALT1*x2),(*BCL2*x2),(*BCL3*x2),(*IGK*x2)	*2q22.1*[§§]	11q22.2-q23.3	

Table 1 (continued)

2-R2[¶¶]	Pos	Break, non-IG	††	9p24.3-p22.3	4q24, 4q34.1-q34.2, 8q21.3, 8q24.21, 11q22.2-q23.3, 11q24.3	
3	Pos	Break, *MYC con CCND1 con IGH*	50,XY,+X,dup(1)(q21q31),+5,+9,t(11;14)(q13;q32),+12,+21[5]/50,idem,der(8)t(8;14)(q24;q32)t(11;14),der(11)t(11;14),der(14)t(8;14)[3]/46,XY[16]. Ish der(?3)(IGH+)[3],t(11;14)(*CCND1*+,IGH+;IGH+,*CCND1*+)[3] nuc ish(3′*BCL6*,5′*BCL6*)x2(3′*BCL6* sep 5′*BCL6*x1),(*BCL6*,IGH)x3 (*BCL6* con IGHx1),(*MYC*x2),(*MYC*x2, *CCND1*x3,IGHx4)(*CCND1* con IGHx2), (5′*CCND1*,3′*CCND1*)x2 (5′*CCND1* sep 3′*CCND1*x1), (*CCND1*x3,IGHx4) (*CCND1* con IGHx2)/(5′*MYC*,3′*MYC*) x2(5′*MYC* sep 3′*MYC*x1), (*MYC*x3,*CCND1*x3, IGHx5) (*MYC* con *CCND1* con IGHx1)(*MYC* con IGHx1)(*CCND1* con IGHx1), (5′*CCND1*,3′*CCND1*)x2 (5′*CCND1* sep 3′*CCND1*x1), (*CCND1*x3,IGHx5) (*CCND1* con IGHx1)	1q21.3-q32.2, 1q32.3-q44, 5p15.33-q35.3, 9p24.3-p21.3, 9p21.3-p11.2, 11q24.3, 12p13.33-q24.33, *14q23.1-q23.2,* 21p11.2-q22.3	9p21.3, 9q13-q21.11	10p15.3-p11.1, 10q11.21--q26.3, 18q21.33-q23, 20p13-q13.33
4	Pos	Break, IGH-*MYC*, *MYC* con *CCND1* con IGH	*CDKN2A/B* homozygous deletion			
5	Pos	Break	IGH-*MYC*, IGK-*MYC*, IGL-*MYC*, *MYC-PAX5*, *BCL6-MYC* : all negative	3q25.31-q29, 7p22.3-q11.23, 7q11.23-q36.1, 7q36.1-q36.3, 8p23.3-q24.3, 9q21.11-q21.31, 9q21.31-q22.31, 11q13.3-q25, 13q31.3, 13q31.3-q32.1, 14q23.3-q32.33, 16p13.3-q24.3	4p16.3-q35.2, 6p25.3-q27, 9p24.3-13.1, 9q33.3-q34.3, 13q32.1-q34, 15q11.1-q22.2, 17p13.3-p11.2, 18p11.32-q23, 19p13.3-q13.43	9q22.31-q33.3, 13q11-q31.3
6	Pos	Break[§§§]	¶¶¶	3q25.31-q26.31, 3q26.32, 3q27.2-q29, 7p22.3-p14.1, 8q23.1-q24.3, 12p13.33-p11.1, 21q21.2-q22.3	1p13.3-p11.2, 1q23.1-q31.3, 1q32.3-q41,1q41, 1q42.3-q44, 2q36.2-q37.3, 3p26.3-p26.1, 6p12.3-q27, 8p23.3-p11.23, 8q12.1-q13.3, 9p23-p13.1, 12q11-q12, 12q12-q13.11, 13q32.1-q34, 15q26.1-q26.3, 20q11.21-q13.12	3q26.32-q27.2
6-R	Pos	Break, *MYC-PAX5*	¶¶¶	1p32.3-p31.3, 1p31.3-p31.1, 2q22.1-q35, 3q25.31-q29,	1p36.12-p36.11, 1p32.3, 1p13.3-p11.2, 2q35-q37.3, 3p26.3-p26.1, 3p14.2,	

Table 1 (continued)

				7p22.3-p14.1, 7q35-q36.3, 8q24.21, 18q21.2-q23	9p22.1-p21.3, 9p21.3-p21.2, 9p21.2-q31.3, 11q24.2-q25, 15q26.1-q26.3, 20q11.21-q13.12
7	Pos	Atypical break[††††], *MYC* con *CCND1* con IGH	45,XY,−4,der(8)t(8;11)(q24;q13),der(13)t(11;13)(p12;p11),der(14)t(8;14)(q24;q32),der(17)t(4;17)(q13;p12)[7]/44,idem,der(8;22)(q10;q10),del(9)(p21)[10] nuc ish (5′*MYC*x3,3′*MYC*x2)(5′*MYC* con 3′*MYC*x2),(*MYC*x3, *CCND1*x4,IGHx3 ~ 4)(*MYC* con *CCND1* con IGHx2), (*CDKN2A*x1, D9Z1x2),(D11Z1x2,*ATM*x3,*FDX*x3),(*CCND1*x4,IGHx3)(*CCND1* con IGHx2),(DDIT3x2),(D13S319,D13S25)x2,(3′IGHx3,5′IGHx1)(3′IGH con 5′IGHx1),(*P53*x1,*MPO*x2) ish der(8)t(8;11)(*MYC*+,IGH+,*CCND1*+)[5],(3′*CCND1*+)[6],(*ATM*+,*FDX*+)[3],(3′IGH+)[6],(IGH+,*CCND1*+)[3],del(9)(p21)(*CDKN2A*−,D9Z1+)[2],der(14)t(8;14)(3′*MYC*+)[2],(3′*MYC1*+)[4],(IGH+,*CCND1*+,*MYC*+)[5],(3′*CCND1*+)[6], (3′IGH+,5′IGH−)[6],(IGH+,*CCND1*+)[3],der(17)t(4;17)(*P53*−,*MPO*+)[3]		
8	Pos	Break	IGH-*MYC*, IGK-*MYC*, IGL-*MYC*, *MYC-PAX5*, *BCL6-MYC* : all negative		
9	Pos	Break	IGH-*MYC*, IGK-*MYC*, IGL-*MYC*, *MYC-PAX5*, BCL6-*MYC* : all negative		
10	Pos	Break[‡‡‡‡]	*BCL6* break, *BCL2* negative		
11	Pos	Break[‡‡‡‡]			
12	Pos	Break	IGH-*MYC*, IGK-*MYC*, IGL-*MYC*, *MYC-PAX5*, *BCL6-MYC* : all negative		
13	Pos	IGL-*MYC*[¶¶¶¶]	47,XX,+7,t(8;22)(q24;q11),der(9)t(3;9)?(q13;p2?3)x2,der(11)t(1;11)(q21;q13)ins(11;?)(q13;?),t(11;14)(q13;q32),der(13)t(8;13)(q22;q3?2)t(8;22)(q24;q11)/[9]/46,XX[3]		

B blastoid, *BMB* bone marrow biopsy, *CB* centroblastic, *C* classic, *CN* copy number, *CNN-LOH* copy number neutral loss of heterozygosity, *CNV* copy number variant, *con* connected signals, *cyto* cytology, *F* female, *IB* immunoblastic, *LN* lymph node, *M* male, *Mo* month, *NA* not analysed, *No* number, *PB* peripheral blood, *Pleo* pleomorphic, *P* polymorph, *sep* separated signals, *Sp* spleen

[*] Intrinsic to the different techniques used (FISH, karyotyping and array-based CNV analysis), not all aberrations are detected by all three techniques [23]. For array-based CNV analysis, affected cytobands are listed

[†] Case no. 1 analysed by array-CGH, all other cases by Oncoscan™. Only aberrations other than those involving the IGH/IGK/TCR-loci and sex-chromosomes are included

[‡] Positive by conventional cytogenetics and/or FISH (*CCND1* break-apart and/or *IGH-CCND1* dual-fusion or *IGH-CCND1-MYC* tricolor FISH probe)

[§] If not stated otherwise, break refers to break determined by FISH

[¶] In case the *MYC* partner has been identified, negative FISH results for other translocation partners are not listed for readability

[**] CNV profile from array-CGH, intrinsic to the applied methodology, LOH not determined in this case

[††] Clonal relationship confirmed by clonality analysis

[‡‡] Complete FISH results: nuc ish 1p22 (*BCL10* prox × 2, *BCL10* dist × 2), 3q27 (*BCL6* prox × 2, *BCL6* dist × 2), 11 (CEP11 × 2, *CCND1* × 3, *ATM* × 1, *FDX* × 1), 12q13 (*CHOP* prox × 2, *CHOP* dist × 2), 13q14 (D13S319 × 2, D13S25 × 2), 14q32 (IGH × 3, IGH prox × 2, IGH dist × 2), 17 (*P53* × 2, CEP17 × 2), 18q21 (*MALT1* prox × 2, *MALT1* dist × 2)(*BCL10* prox sep *BCL10* dist × 0)(*BCL6* prox sep *BCL6* dist × 0)(IGH con *CCND1* × 2)(IGH prox sep IGH dist × 1)(*MALT1* prox sep *MALT1* dist × 0)

[§§] Subclonal aberrations are italicized

[¶¶] Case included in tissue microarray in Dai et al [8]

[***] Array analysis performed on DNA extracted from decalcified FFPE BM-trephine. Forty percent blasts in peripheral blood

[†††] Additional immunohistochemical stainings CD38−, CD138−, MUM1+

[‡‡‡] Patient suspected of having a hematologic malignancy of mature monoclonal B-cells (B-CLL/B-PLL or potentially leukemic MCL[24]) on evaluation with flow-cytometry 3–4 years earlier (CD19+, CD20+, CD5+, CD22+, CD23+/−, CD38+, CD79+/−, CD10−, CD11C−, CD25−, CD43−, CD103−, FMC7+/−, IgM+, ZAP70−)

[§§§] Complex rearrangement. *MYC-PAX5* fusion not confirmed by FISH in this sample

[¶¶¶] Clonal relationship confirmed by clonality analysis

[****] IGH-*MYC* and IGH-*CCND1* confirmed by FISH in the BM biopsy analysed for MYC expression

[††††] Atypical break with two co-localisations and one additional red signal by analysis with *MYC* break-a-part probe

[‡‡‡‡] No material available for evaluation of *MYC* translocation partner

[§§§§] Leukemic, no peripheral lymphadenopathy. Immunophenotyping by flow-cytometry on peripheral blood (FCM markers CD5+/−, CD10+/−, CD11c−, CD19+, CD20++, CD22+/−, CD23−, CD24+/−, CD25+/−, CD103−, FMC7++, s-IgM+, S-IgD−, s-IgG−, s-IgA−, s-Kappa+, s-Lambda−). No immunohistochemistry available

[¶¶¶¶] No *MYC* break detected with commercially available *MYC* BAP. Far telomeric break detected with home-brew *MYC*-3 probe. IGL-*MYC* fusion confirmed by FISH

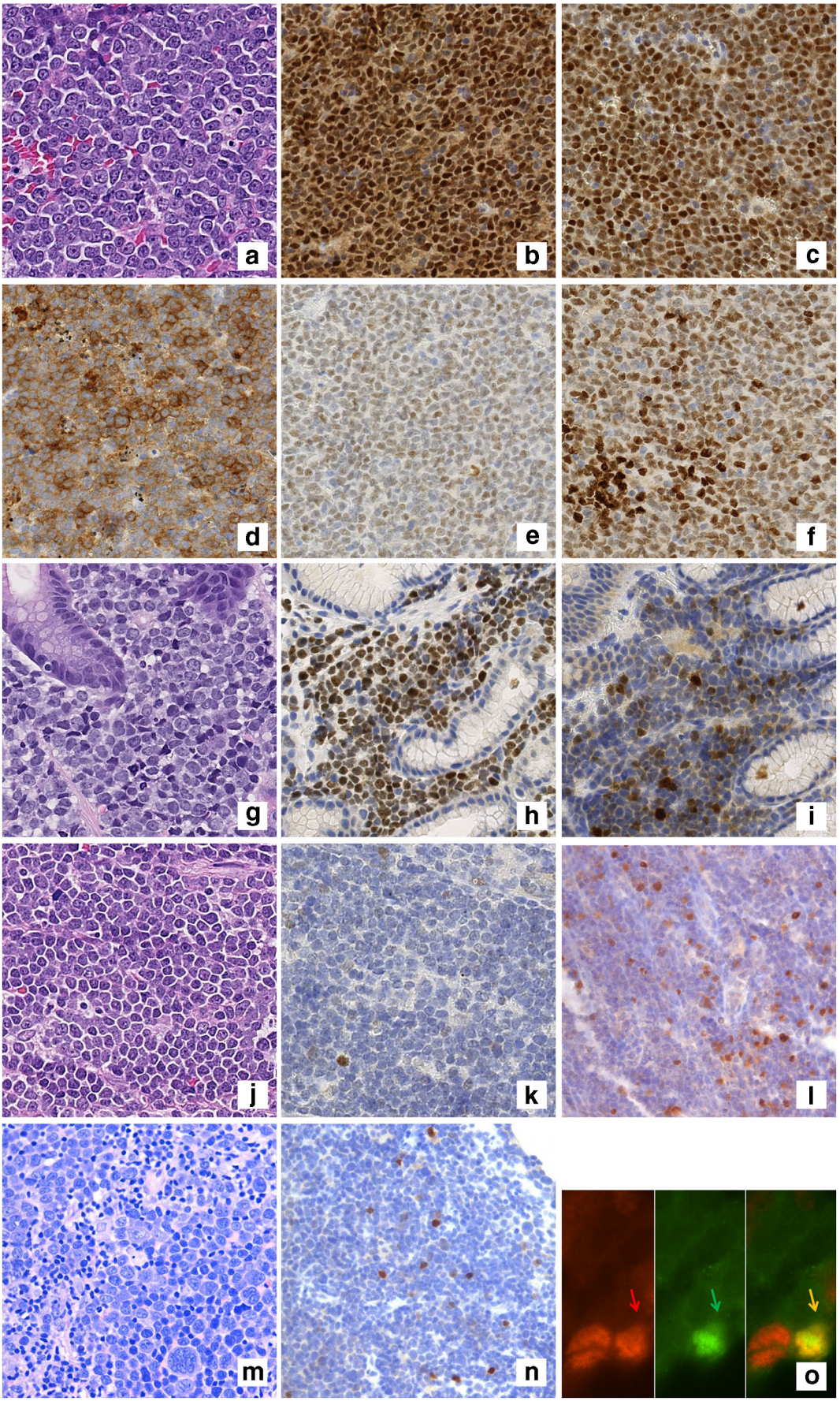
a
b
c
d
e
f
g
h
i
j
k
l
m
n
o

◀ **Fig. 1** Morphological and immunophenotypic characteristics. A prototypical case (nr. 8) is shown in panels **a–f**, featuring a DLBCL-like, immunoblastic cytologic appearance (**a** HE, × 40), a MCL phenotype (**b** cyclin-D1, × 40 and **c** SOX11, × 40), co-expression of CD10 (**d** × 40) and BCL6 (**e** × 40) and substantial positivity for MYC (non-IG *MYC* rearrangement) (**f** × 40). TdT-expressing cases are further depicted. Case 4 features a blastoid appearance (**g** HE, × 40) and a lymphoblastic lymphoma-like phenotype, including SOX11 expression (**h** × 40) and partial TdT-positivity (**i** × 40), but with IGH-*CCND1*, with cyclin D1 overexpression (not shown), and IGH-*MYC*. Case 6-R which harbours IGH-*CCND1* and *MYC-PAX5* fusion shows blastoid to Burkitt-like cytology (**j** HE, × 40), scant SOX11 reactivity (**k** × 40) with a minor component of TdT-positive cells (**l** × 40). Case 5 shows pleomorphic morphology with occasionally anaplastic cells (**m** × 40) and intermingled single TdT-positive cells (**n** × 40) which were shown to be cyclin-D1/TdT double positive cells (**o** × 100, cyclin-D1 red, TdT green, double-positive cells yellow)

hg19). OncoScan™ analysis was performed on the cases with available material and multiple time points available (cases 2 and 6), with TdT-expression (cases 5 and 6R) and case 3. A high chromosomal complexity was defined as having ≥ 6 aberrations by array-based CNV analysis [15].

Results

Epidemiological and clinical characteristics

The great majority of the patients were male 11/13 (85%). Mean age at diagnosis was 68 years (range: 53–83 years). A predominance of the samples was from extra-nodal sites (10/15, 67%).

Histopathological and immunophenotypic characteristics

Since the first sample of patient 2 was *MYC*-break negative, this sample was only used for clonal evolution analysis. The majority of *MYC* − R+ samples (13/15, 87%) presented with non-classic cytology in particular blastoid (n = 8). The five pleomorphic cases featured a cytology ranging from centroblastic to immunoblastic and anaplastic (Fig. 1a, g, j, m, Table 1). A small cell cytology was observed in case 7. In two patients, sequential biopsies were available: in patient 2, the cytology was classic in the initial diagnostic (*MYC* − R −) and first-relapse sample (*MYC* − R+) and blastoid at second relapse (*MYC* − R+). Both biopsies of patient 6 had an aggressive cytology (pleomorphic and blastoid). SOX11 was negative or only focally expressed in 4/14 samples (28%, Fig. 1c, h, k and Table 1) while 10/15 (67%) samples displayed at least minor expression of CD10 and/or BCL6 (Fig. 1d, e and Table 1). Of note, foci or focal and in case 4 more diffuse expression of TdT − positive cells (≥ 2–20%) was detected in 3 out of 13 samples (23%) tested (Fig. 1i, l, n, Table 1). A blastoid morphology was seen in 2/3 TdT+ cases (cases 4 and 6-R) while case 5 had a pleomorphic histology with anaplastic cells. To determine the nature of these TdT-positive cells, we performed cyclin-D1-TdT immunofluorescence double staining in cases 5 and 6-R which revealed that TdT was expressed

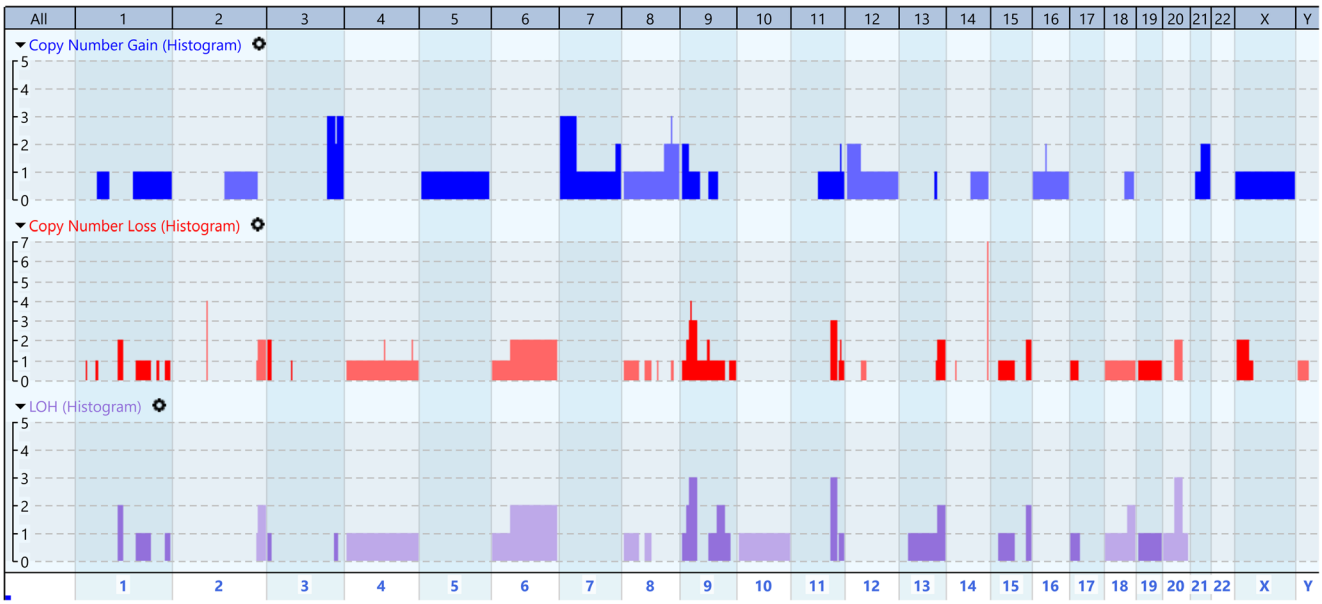

Fig. 2 Landscape of combined genomic copy number gains (dark blue), losses (red) and loss-of-heterozygosity (LOH, purple) of cases 2 (initial diagnosis, first- and second relapse), 3, 5 and 6 (initial diagnosis and relapse). CNVs of case 1 (array-CGH) are not depicted in the figure. The Y-axis depicts the absolute number of samples with the respective aberration. Focal CN aberrations may not be visible in the figure. Genomically distinct aberrations but within close proximity of each other may not be visible as separate but instead as single genomic event. LOH includes both LOH resulting from deletions and from copy number neutral loss of heterozygosity. Not all deletions may be displayed also in the LOH histograms and vice versa as for copy number loss and LOH different calling algorithms are used

by a subset of cyclin-D1 positive cells (Fig. 1o). Using a cut-off of ≥ 40% positive cells [6], MYC was expressed in 12/13 (92%) samples. P53 was expressed by all *MYC* − R+ samples tested (13/13, 100%) with 6/13 (46%) showing high expression (> 50% of lymphoma cells). Ki-67 was high (≥ 30%) in 12/13 (92%) samples, ≥ 75% in 7/13 (54%) samples and in 3 patients ≥ 90%. In both patients with sequential biopsies available, there was an increase in the Ki-67 proliferation index (18%, diagnostic *MYC* − R negative sample, 53% and 90% for patient 2 and 54% and 77% for patient 6).

Conventional and molecular cytogenetics

In 11/13 patients, the *MYC* − translocation partner could be investigated by conventional and/or molecular cytogenetics. In 4/11 patients, the *MYC* − translocation partner was one of the IG-loci (Table 1) as determined by karyotyping and FISH (case 7, IGH-*MYC* ; case 13 IGL-*MYC*), FISH (case 4, IGH-*MYC*) or karyotyping (case 3, der(8)t(8;14)(q24;q32)t(11;14)). In 7/11 cases, the *MYC* − translocation partner was a non-IG partner. In cases 1 and 6-R, there was a *PAX5/MYC* (9p13/8q24) fusion by FISH while in cases 2-R2, 5, 8, 9 and 12, no *MYC* − partner could be identified with the applied FISH assays (Table 1). All patients with conventional cytogenetics available had karyotypes with ≥ 3 aberrations.

Array-based copy number variant analyses

Array-based copy number variant (CNV) analysis was available for eight samples from five patients including for two patients at multiple time points. The copy number variants for the individual cases are listed in Table 1 and visualised in Fig. 2. The most common (subclonal) aberration (other than those involving the IGH/IGK/TCR-Loci and sex-chromosomes) was loss of 9p21.3 involving *CDKN2A/CDKN2B* occurring in 4 patients and 5 samples with a homozygous deletion in sample 6-R. Other common aberrations included (focal) gains of chromosome 3q including the *BCL6* locus at 3q27.3 in samples 5, 6 and 6R, 7p (1, 5, 6 and 6R), 7q (1, 5 and 6R) and 8q including the 8q24.21/*MYC*-locus (1, 5, 6 and 6R). The *ATM* locus at 11q22.3 and *TP53* locus at 17p13.1 were deleted in patient 2 (diagnosis and relapses) and 5 respectively.

Clonal evolution

In patients 2 and 3, the clonal evolution of *MYC* − breaks could be assessed. In both patients, subclones with and without the *MYC* − break were present in the obtained karyotypes. In addition, the *MYC* − break was absent in the diagnostic biopsy of patient 2. From patients 2 and 6, biopsies from multiple time-points could be analysed by OncoScan™. The individual CNV-profiles of the diagnostic and relapse samples of patients 2 and 6 are shown in supplementary Figs. 1 and 2 respectively. In patient 2, a deletion of ≈ 13–14 Mb at 11q22.2-q23.3 involving the *ATM* locus was present in the initial diagnostic and both relapse samples. Together with the *MYC*-break, gains at 9p and losses at 4q and 8q were acquired during disease progression indicative of a linear clonal evolution pattern at the level of array-based CNV analysis. Both biopsies of patient 6, at initial diagnosis and relapse, showed complex aberrations sharing various alterations but each also having a set of unique ones. In the initial diagnostic biopsy, there was a heterozygous deletion of chromosomal locus 9p21.3 involving *CDKN2A/CDKN2B* while there was a homozygous deletion of this locus at relapse. Overall, all *MYC* − positive samples (except 2R1) showed complex genomic landscapes as defined as having ≥ 6 aberrations by array-based CNV analysis [15].

Discussion

In the present study, we performed a comprehensive histopathological and molecular-(cyto)genetic characterization of a (considering the rarity of these lymphomas) large series of MCL with *CCND1*− and *MYC* − breaks. Unusual but previously reported findings were a DLBCL-like cytology with expression of CD10 and/or BCL6 [10, 25, 26], relatively frequent SOX11 negativity and recurrent (focal) positivity for TdT, all features posing a diagnostic challenge. However, it has to be taken into account that the cases included in the present study were collected from reference pathology centres and genetic laboratories and may therefore be enriched for unusual clinical, morphological, immunophenotypic and/or genetic features. The DLBCL−like cytology (ranging from centroblastic to immunoblastic and including anaplastic) and immunophenotypic features (i.e. expression of CD10 and/or BCL6) may prompt an incorrect diagnosis of DLBCL or high grade B-cell lymphoma unless cyclin-D1 staining and/or FISH for *CCND1* − break is performed [10, 25, 27]. This issue could be particularly pertinent to cases 3, 6-R, 7 and 11 which also showed negative to weak expression of SOX11 (see below).

Approximately 30% of the cases in the present study—two of which were diagnosed on bone marrow biopsies—were SOX11 negative or only focally positive. This SOX11 negativity rate is markedly higher than reported by Nygren et al. [28] and in a series of 344 (predominantly nodal) MCL from clinical trials of the European Mantle Cell Lymphoma Network (EMCL) in which only 9/344 (3%) and 16/344 (5%) were SOX11 expression negative and low, respectively [18]. Importantly, in this latter study, no correlation between negative/low SOX11 expression and Ki67 was found [18] and amongst 250 patients from this study with both cytology information and SOX11 expression data, though not reaching

statistical significance, a difference was observed in the percentage of patients with blastic cytology in the SOX11 IHC negative, low and high groups. This was slightly higher in the group with negative or low SOX11 IHC than in those with SOX11 > 10% (17% and 18% versus 10%, p value for 3-group comparison $p = 0.31$, data not shown). Whether these differences really exist needs to be investigated in larger cohorts.

Although previously reported in three individual cases [11, 14, 29], we observed recurrent TdT positivity in 3/13 samples with pleomorphic/blastoid morphology ranging from focally positive cells (cases 5 and 6-R) to more pronounced staining (20%, case 4). As assessed by cyclin-D1 and TdT immunofluorescence, double staining in two cases TdT was expressed by a subpopulation of the lymphoma cells themselves, thus excluding the possibility of homing of benign precursors [30]. In case 4, no material was available for double-staining but in this case, the percentage of TdT-positive cells (20%) far outnumbered a possible small non-neoplastic cell population. Aberrant expression of TdT, which is usually only expressed in precursor B- and T-cells and neoplasms derived from these cells and also in AML-M0 [12–14], has been occasionally reported in high-grade B-cell lymphomas and only in three other MCL [11, 14, 29]. The case published by Kallen et al. [11] had a component with conventional morphology lacking both an *MYC* − rearrangement and TdT expression as well as a blastic component with a *MYC* − rearrangement and TdT expression. In the series of 17 MCL with a dual rearrangement of *CCND1* and *MYC*, all three cases that had been tested for TdT expression were negative [9]. The mechanism by which TdT is (re-)expressed is unknown but it may be similar to the phenomenon in rare cases of (transformed) follicular lymphoma with a dual rearrangement of *BCL2* and *MYC* [31]. Likely, it is a secondary phenomenon, also supported by our observations in case 6, where the first sample did not show any TdT expression whereas the second sample showed positivity in less than 5% of the cells. In addition, in case 4, there was a history of a (unspecified) haematological disease. This is in line with the case published by Ok et al. [14] which also had a history of MCL and in the case reported by Cantu et al. [29], there was in addition to the TdT positive nodal blastic MCL a typical MCL involving the bone marrow. Independent of this, TdT expression in MCL seems to be uncommon as 0/15 blastoid/pleomorphic MCLs (previously assessed for MYC expression [8]) showed TdT positivity and in a series of 112 MCL published by Zhou et al., all were TdT negative [32].

The acquisition of *MYC* − break likely occurs secondary to the *CCND1* − rearrangement (as exemplified by patients number 2 and 3) and parallels the observation in transformed follicular lymphomas [6, 31, 33]. In addition, this sequence of events is supported by the observation that the *t*(11;14)/IGH-*CCND1* occurs mostly at pre-B-cell stage ([34] and reviewed in [35]) while *MYC* − rearrangements occur (with very rare exceptions[12]) in the germinal centre [3]. Although the retrospective nature and the aforementioned referral bias of this study hinder a 'true' estimate about the frequency of *MYC* − breaks in MCL, *MYC* − breaks in this entity seem to be rare: approximately 5% of MCL with published conventional cytogenetic data harbour an additional 8q24/*MYC* breakpoint [7]—this relatively high frequency is likely influenced by referral and publication bias—while the frequency seems lower in our previously published series of tissue micro-arrays composed of unselected cases (0/55 for classical MCL) but comparable for pleomorphic/blastic MCL (1/19, 5%) [8]. In the series by Hu et al., *MYC* − rearrangements were detected in 17/1162 cases (1.5%) of MCL [9] and in 4/126 (3,2%) by Malarikova [36].

An interesting observation was the high frequency of (focal) copy number (CN) deletions of the *CDKN2A* locus (9p21.3) in 4/5 patients evaluated by array-based CNV analysis and 2/2 by FISH. This incidence is markedly higher than previously reported (20% in [37], 7–30%, reviewed in [38] and 18–41%, reviewed in [39], 33% in [36]) but in line with the recently reported hetero- and homozygous CN loss of *CDKN2A/B* in 12/13 (92%) of pleomorphic/blastoid MCL [40]. Other CN abnormalities which were detected by array-based CNV analysis have been reported as recurrent previously [38]. The current study showed a high frequency of 'high-grade' pathological features in MCL with concomitant *MYC* and *CCDN1* breaks including pleomorphic/blastoid morphology, frequent P53 expression, *CDKN2A* deletions, high Ki-67 proliferation index and a high genomic complexity, all biological features associated with aggressive disease and poor prognosis [18, 36, 39–41]. These findings challenge the development of innovative therapeutic approaches for the (mostly elderly) patients with MCL and *MYC* − breaks [1, 42] as the presence of a *MYC* − break may have, even amongst already aggressive blastoid MCL, additional unfavourable prognostic impact [10].

Supplementary Information The online version contains supplementary material available at https://doi.org/10.1007/s00428-021-03022-8.

Authors' contributions S.M.A., G.A.C., R.S. and W.K. designed the research; G.O., A.R., E.v/d B., A.B-B., M.H., I.B., E.H., M.K., W.B. S.J. and M.J.S.D. provided clinical, genetic and/or pathological data and samples; S.M.A, R.W., S.B., K.O-H., M.K., J.B., I.N., E.M.P. and R.S. performed (molecular)cytogenetic, molecular and/or bio-informatical analyses; G.A.C., P.K., I.O. and W.K. performed histopathological review; S.M.A., G.A.C., R.S. and W.K. wrote the manuscript; all authors approved the final version of the manuscript.

Funding The research of W.K. and R.S. on MYC positive lymphomas is supported in the framework of a MMML-MYC-SYS grant (036166B) by the German Ministry of Science and Education (BMBF). Former grant support of MMML by the Deutsche Krebshilfe (2003–2011) and the support of the technical staff of the Institutes of Human Genetics in Kiel and Ulm are gratefully acknowledged. Work in Leicester supported

by Cancer Research UK in conjunction with the UK Department of Health on an Experimental Cancer Medicine Centre grant [C10604/A25151].

Compliance with ethical standards

Conflict of interest The authors declare that they have no conflict of interest.

Ethics approval The study was conducted in accordance with the recommendations of the ethics board of the Medical Faculty, University of Kiel, numbers D425/03, D447/10 and amendment from 09.03.2010 which includes that based on the historic nature of several cases a written informed consent on participation and publication could not be obtained.

Consent to participate See the 'Ethics approval' section.

Consent for publication See the 'Ethics approval' section.

Code availability NA

References

1. Dreyling M, Klapper W, Rule S (2018) Blastoid and pleomorphic mantle cell lymphoma: still a diagnostic and therapeutic challenge! Blood 132:2722–2729. https://doi.org/10.1182/blood-2017-08-737502
2. Sander B, Quintanilla-Martinez L, Ott G, Xerri L, Kuzu I, Chan JKC, Swerdlow SH, Campo E (2016) Mantle cell lymphoma–a spectrum from indolent to aggressive disease. Virchows Arch 468:245–257. https://doi.org/10.1007/s00428-015-1840-6
3. López C, Kleinheinz K, Aukema SM et al (2019) Genomic and transcriptomic changes complement each other in the pathogenesis of sporadic Burkitt lymphoma. Nat Commun 10:1459. https://doi.org/10.1038/s41467-019-08578-3
4. Christie L, Kernohan N, Levison D, Sales M, Cunningham J, Gillespie K, Batstone P, Meiklejohn D, Goodlad J (2008) C-MYC translocation in t(14;18) positive follicular lymphoma at presentation: an adverse prognostic indicator? Leuk Lymphoma 49:470–476. https://doi.org/10.1080/10428190701836845
5. Ziemba JB, Wolf Z, Weinstock M, Asakrah S (2020) Double-hit and triple-hit follicular lymphoma. Am J Clin Pathol 153:672–685. https://doi.org/10.1093/ajcp/aqz208
6. Aukema SM, van Pel R, Nagel I, Bens S, Siebert R, Rosati S, van den Berg E, Bosga-Bouwer AG, Kibbelaar RE, Hoogendoorn M, van Imhoff GW, Kluin-Nelemans HC, Kluin PM, Nijland M (2017) MYC expression and translocation analyses in low-grade and transformed follicular lymphoma. Histopathology 71:960–971. https://doi.org/10.1111/his.13316
7. Aukema SM, Siebert R, Schuuring E, van Imhoff GW, Kluin-Nelemans HC, Boerma EJ, Kluin PM (2011) Double-hit B-cell lymphomas. Blood 117:2319–2331. https://doi.org/10.1182/blood-2010-09-297879
8. Dai B, Grau M, Juilland M, Klener P, Höring E, Molinsky J, Schimmack G, Aukema SM, Hoster E, Vogt N, Staiger AM, Erdmann T, Xu W, Erdmann K, Dzyuba N, Madle H, Berdel WE, Trneny M, Dreyling M, Jöhrens K, Lenz P, Rosenwald A, Siebert R, Tzankov A, Klapper W, Anagnostopoulos I, Krappmann D, Ott G, Thome M, Lenz G (2017) B-cell receptor–driven MALT1 activity regulates MYC signaling in mantle cell lymphoma. Blood 129:333–346. https://doi.org/10.1182/blood-2016-05-718775
9. Hu Z, Medeiros LJ, Chen Z, Chen W, Li S, Konoplev SN, Lu X, Pham LV, Young KH, Wang W, Hu S (2017) Mantle cell lymphoma with MYC rearrangement: a report of 17 patients. Am J Surg Pathol 41:216–224. https://doi.org/10.1097/PAS.0000000000000758
10. Wang L, Tang G, Medeiros LJ, Xu J, Huang W, Yin CC, Wang M, Jain P, Lin P, Li S (2020) MYC rearrangement but not extra MYC copies is an independent prognostic factor in patients with mantle cell lymphoma. Haematologica.:haematol.2019.243071. https://doi.org/10.3324/haematol.2019.243071
11. Kallen ME, Rao NP, Kulkarni SK, Pullarkat ST, Said J, Tirado CA, Ahmed RS, Miller JM, Chung PY, Kahn DG, Song SX (2015) B-lymphoblastic transformation of mantle cell lymphoma/leukemia with "double hit" changes. J Hematop 8:31–36. https://doi.org/10.1007/s12308-014-0229-9
12. Wagener R, López C, Kleinheinz K, Bausinger J, Aukema SM, Nagel I, Toprak UH, Seufert J, Altmüller J, Thiele H, Schneider C, Kolarova J, Park J, Hübschmann D, Murga Penas EM, Drexler HG, Attarbaschi A, Hovland R, Kjeldsen E, Kneba M, Kontny U, de Leval L, Nürnberg P, Oschlies I, Oscier D, Schlegelberger B, Stilgenbauer S, Wössmann W, Schlesner M, Burkhardt B, Klapper W, Jaffe ES, Küppers R, Siebert R (2018) IG-*MYC*$^{+}$ neoplasms with precursor B-cell phenotype are molecularly distinct from Burkitt lymphomas. Blood 132:2280–2285. https://doi.org/10.1182/blood-2018-03-842088
13. Patel KP, Khokhar FA, Muzzafar T, James You M, Bueso-Ramos CE, Ravandi F, Pierce S, Medeiros LJ (2013) TdT expression in acute myeloid leukemia with minimal differentiation is associated with distinctive clinicopathological features and better overall survival following stem cell transplantation. Mod Pathol 26:195–203. https://doi.org/10.1038/modpathol.2012.142
14. Ok CY, Medeiros LJ, Thakral B, Tang G, Jain N, Jabbour E, Pierce SA, Konoplev S (2019) High-grade B-cell lymphomas with TdT expression: a diagnostic and classification dilemma. Mod Pathol 32:48–58. https://doi.org/10.1038/s41379-018-0112-9
15. Hummel M, Bentink S, Berger H, Klapper W, Wessendorf S, Barth TFE, Bernd HW, Cogliatti SB, Dierlamm J, Feller AC, Hansmann ML, Haralambieva E, Harder L, Hasenclever D, Kühn M, Lenze D, Lichter P, Martin-Subero JI, Möller P, Müller-Hermelink HK, Ott G, Parwaresch RM, Pott C, Rosenwald A, Rosolowski M, Schwaenen C, Stürzenhofecker B, Szczepanowski M, Trautmann H, Wacker HH, Spang R, Loeffler M, Trümper L, Stein H, Siebert R (2006) A biologic definition of Burkitt's lymphoma from transcriptional and genomic profiling. N Engl J Med 354:2419–2430. https://doi.org/10.1056/NEJMoa055351
16. Aukema SM, Kreuz M, Kohler CW, Rosolowski M, Hasenclever D, Hummel M, Kuppers R, Lenze D, Ott G, Pott C, Richter J, Rosenwald A, Szczepanowski M, Schwaenen C, Stein H, Trautmann H, Wessendorf S, Trumper L, Loeffler M, Spang R, Kluin PM, Klapper W, Siebert R, for the Molecular Mechanisms in Malignant Lymphomas (MMML) Network Project (2014) Biological characterization of adult MYC-translocation-positive mature B-cell lymphomas other than molecular Burkitt lymphoma. Haematologica 99:726–735. https://doi.org/10.3324/haematol.2013.091827
17. Klapper W, Hoster E, Determann O et al (2009) Ki-67 as a prognostic marker in mantle cell lymphoma—consensus guidelines of the pathology panel of the European MCL Network. J Hematop 2:103–111. https://doi.org/10.1007/s12308-009-0036-x
18. Aukema SM, Hoster E, Rosenwald A, Canoni D, Delfau-Larue MH, Rymkiewicz G, Thorns C, Hartmann S, Kluin-Nelemans H, Hermine O, Dreyling M, Klapper W (2018) Expression of TP53 is associated with the outcome of MCL independent of MIPI and Ki-67 in trials of the European MCL Network. Blood 131:417–420. https://doi.org/10.1182/blood-2017-07-797019

19. Croci GA, Hoster E, Bea S et al (2020) Reproducibility of histologic prognostic parameters for mantle cell lymphoma: cytology, Ki67, p53 and SOX11. Virchows Arch 477:259–267. https://doi.org/10.1007/s00428-020-02750-7
20. McGowan-Jordan J, Simons A, Schmid M (Eds) (2016) ISCN 2016 An international system for human cytogenomic nomenclature. Karger, Basel.
21. Aukema SM, Theil L, Rohde M, Bauer B, Bradtke J, Burkhardt B, Bonn BR, Claviez A, Gattenlöhner S, Makarova O, Nagel I, Oschlies I, Pott C, Szczepanowski M, Traulsen A, Kluin PM, Klapper W, Siebert R, Murga Penas EM (2015) Sequential karyotyping in Burkitt lymphoma reveals a linear clonal evolution with increase in karyotype complexity and a high frequency of recurrent secondary aberrations. Br J Haematol 170:814–825. https://doi.org/10.1111/bjh.13501
22. Martin-Subero JI, Harder L, Gesk S et al (2002) Interphase FISH assays for the detection of translocations with breakpoints in immunoglobulin light chain loci. Int J Cancer 98:470–474. https://doi.org/10.1002/ijc.10169
23. Kluin P, Schuuring E (2011) Molecular cytogenetics of lymphoma: where do we stand in 2010? Histopathology 58(1):128–144. https://doi.org/10.1111/j.1365-2559.2010.03700.x
24. Craig FE, Foon KA (2008) Flow cytometric immunophenotyping for hematologic neoplasms. Blood 111(8):3941–3967. https://doi.org/10.1182/blood-2007-11-120535
25. Pizzi M, Agostinelli C, Righi S, Gazzola A, Mannu C, Galuppini F, Fassan M, Visentin A, Piazza F, Semenzato GC, Rugge M, Sabattini E (2017) Aberrant expression of CD10 and BCL6 in mantle cell lymphoma. Histopathology 71:769–777. https://doi.org/10.1111/his.13286
26. Xu J, Medeiros LJ, Saksena A et al (2018) CD10-positive mantle cell lymphoma: clinicopathologic and prognostic study of 30 cases. Oncotarget 9:11441–11450. https://doi.org/10.18632/oncotarget.23571
27. Chuang W-Y, Chang H, Chang G-J, Wang TH, Chang YS, Wang TH, Yeh CJ, Ueng SH, Chien HP, Chang CY, Wan YL, Hsueh C (2017) Pleomorphic mantle cell lymphoma morphologically mimicking diffuse large B cell lymphoma: common cyclin D1 negativity and a simple immunohistochemical algorithm to avoid the diagnostic pitfall. Histopathology 70:986–999. https://doi.org/10.1111/his.13161
28. Nygren L, Baumgartner Wennerholm S, Klimkowska M, Christensson B, Kimby E, Sander B (2012) Prognostic role of SOX11 in a population-based cohort of mantle cell lymphoma. Blood 119:4215–4223. https://doi.org/10.1182/blood-2011-12-400580
29. Cantu D, Alvarado Y, Murata-Collins J, Weisenburger DD (2019) Blastic transformation of mantle cell lymphoma with B-lymphoblastic features. Hum Pathol 17:200313. https://doi.org/10.1016/J.EHPC.2019.200313
30. Pizzi M, Brignola S, Righi S, Agostinelli C, Bertuzzi C, Pillon M, Semenzato G, Rugge M, Sabattini E (2018) Benign TdT-positive cells in pediatric and adult lymph nodes: a potential diagnostic pitfall. Hum Pathol 81:131–137. https://doi.org/10.1016/j.humpath.2018.06.027
31. Slot LM, Hoogeboom R, Smit LA, Wormhoudt TAM, Biemond BJ, Oud MECM, Schilder-Tol EJM, Mulder AB, Jongejan A, van Kampen AHC, Kluin PM, Guikema JEJ, Bende RJ, van Noesel CJM (2016) B-lymphoblastic lymphomas evolving from follicular lymphomas co-express surrogate light chains and mutated gamma heavy chains. Am J Pathol 186:3273–3284. https://doi.org/10.1016/j.ajpath.2016.07.027
32. Zhou D-M, Chen G, Zheng X-W, Zhu WF, Chen BZ (2015) Clinicopathologic features of 112 cases with mantle cell lymphoma. Cancer Biol Med 12:46–52. https://doi.org/10.7497/j.issn.2095-3941.2015.0007
33. de Jong D, Voetdijk BM, Beverstock GC et al (1988) Activation of the c-myc oncogene in a precursor-B-cell blast crisis of follicular lymphoma, presenting as composite lymphoma. N Engl J Med 318:1373–1378. https://doi.org/10.1056/NEJM198805263182106
34. Nadeu F, Martin-Garcia D, Clot G, Díaz-Navarro A, Duran-Ferrer M, Navarro A, Vilarrasa-Blasi R, Kulis M, Royo R, Gutiérrez-Abril J, Valdés-Mas R, López C, Chapaprieta V, Puiggros M, Castellano G, Costa D, Aymerich M, Jares P, Espinet B, Muntañola A, Ribera-Cortada I, Siebert R, Colomer D, Torrents D, Gine E, López-Guillermo A, Küppers R, Martin-Subero JI, Puente XS, Beà S, Campo E (2020) Genomic and epigenomic insights into the origin, pathogenesis and clinical behavior of mantle cell lymphoma subtypes. Blood. 136:1419–1432. https://doi.org/10.1182/blood.2020005289
35. Jares P, Colomer D, Campo E (2012) Molecular pathogenesis of mantle cell lymphoma. J Clin Invest 122:3416–3423. https://doi.org/10.1172/JCI61272
36. Malarikova D, Berkova A, Obr A et al (2020) Concurrent TP53 and CDKN2A gene aberrations in newly diagnosed mantle cell lymphoma correlate with chemoresistance and call for innovative upfront therapy. Cancers 12. https://doi.org/10.3390/cancers12082120
37. Eskelund CW, Dahl C, Hansen JW, Westman M, Kolstad A, Pedersen LB, Montano-Almendras CP, Husby S, Freiburghaus C, Ek S, Pedersen A, Niemann C, Räty R, Brown P, Geisler CH, Andersen MK, Guldberg P, Jerkeman M, Grønbæk K (2017) TP53 mutations identify younger mantle cell lymphoma patients who do not benefit from intensive chemoimmunotherapy. Blood 130:1903–1910. https://doi.org/10.1182/blood-2017-04-779736
38. Royo C, Salaverria I, Hartmann EM, Rosenwald A, Campo E, Beà S (2011) The complex landscape of genetic alterations in mantle cell lymphoma. Semin Cancer Biol 21:322–334. https://doi.org/10.1016/j.semcancer.2011.09.007
39. Delfau-Larue M-H, Klapper W, Berger F, Jardin F, Briere J, Salles G, Casasnovas O, Feugier P, Haioun C, Ribrag V, Thieblemont C, Unterhalt M, Dreyling M, Macintyre E, Pott C, Hermine O, Hoster E, European Mantle Cell Lymphoma Network (2015) High-dose cytarabine does not overcome the adverse prognostic value of CDKN2A and TP53 deletions in mantle cell lymphoma. Blood 126:604–611. https://doi.org/10.1182/blood-2015-02-628792
40. Streich L, Sukhanova M, Lu X, Chen YH, Venkataraman G, Mathews S, Zhang S, Kelemen K, Segal J, Gao J, Gordon L, Chen Q, Behdad A (2020) Aggressive morphologic variants of mantle cell lymphoma characterized with high genomic instability showing frequent chromothripsis, CDKN2A/B loss and TP53 mutations: a multi-institutional study. Genes Chromosom Cancer 59:484–494. https://doi.org/10.1002/gcc.22849
41. Rodrigues JM, Hassan M, Freiburghaus C, Eskelund CW, Geisler C, Räty R, Kolstad A, Sundström C, Glimelius I, Grønbæk K, Kwiecinska A, Porwit A, Jerkeman M, Ek S (2020) p53 is associated with high-risk and pinpoints TP53 missense mutations in mantle cell lymphoma. Br J Haematol 191:796–805. https://doi.org/10.1111/bjh.17023
42. Friedberg JW (2017) How I treat double-hit lymphoma. Blood 130:590–596. https://doi.org/10.1182/blood-2017-04-737320

Affiliations

Sietse M. Aukema[1,2] · Giorgio A. Croci[2,3] · Susanne Bens[4] · Kathrin Oehl-Huber[4] · Rabea Wagener[4,5] · German Ott[6] · Andreas Rosenwald[7] · Philip M. Kluin[8] · Eva van den Berg[9] · Anneke G. Bosga-Bouwer[9] · Mels Hoogendoorn[10] · Eva Hoster[11,12] · Iris Bittmann[13] · Inga Nagel[1,14] · Eva M. Murga Penas[1] · Markus Kreuz[15] · Julia Bausinger[4] · Wilfried Belder[16] · Ilske Oschlies[2] · Martin J. S. Dyer[17] · Sandrine Jayne[17] · Reiner Siebert[1,4] · Wolfram Klapper[2]

1 Institute of Human Genetics, Christian-Albrechts University Kiel & University Hospital Schleswig-Holstein, Campus Kiel, Kiel, Germany

2 Hematopathology Section, Christian-Albrechts-University, Kiel, Germany

3 Pathology Unit, Department of Pathophysiology and Transplantation, University of Milan and Fondazione IRCCS, Ca' Granda - Maggiore Policlinico, Milan, Italy

4 Institute of Human Genetics, Ulm University and Ulm University Medical Center, Ulm, Germany

5 Department of Pediatric Oncology, Hematology and Clinical Immunology, University Children's Hospital, Medical Faculty, Heinrich-Heine-University Düsseldorf, Düsseldorf, Germany

6 Department of Clinical Pathology, Robert-Bosch-Krankenhaus, and Dr. Margarete Fischer-Bosch Institute of Clinical Pharmacology, Stuttgart, Germany

7 Institute of Pathology, University of Würzburg, Würzburg, Germany

8 Department of Pathology & Medical Biology, University Medical Center Groningen, Groningen, the Netherlands

9 Department of Genetics, University Groningen, University Medical Centre Groningen, Groningen, the Netherlands

10 Department of Internal Medicine, Medisch Centrum Leeuwarden, Leeuwarden, the Netherlands

11 Institute for Medical Information Processing, Biometry and Epidemiology (IBE), Ludwig-Maximilians-Universität Munich, Munich, Germany

12 Department of Medicine III, University Hospital of the Ludwig Maximilians University Munich, Munich, Germany

13 Institute of Pathology, Agaplesion Hospital Rotenburg, Rotenburg (Wuemme), Germany

14 Institute of Experimental and Clinical Pharmacology, University Hospital Schleswig-Holstein, Campus Kiel, Kiel, Germany

15 Institute for Medical Informatics, Statistics and Epidemiology, University of Leipzig, Leipzig, Germany

16 Pathologie Gütersloh, Gütersloh, Germany

17 Ernest and Helen Scott Haematological Research Institute, University of Leicester, Leicester, UK